CHEMISTRY OF MATERIALS

Article

pubs.acs.org/cm

All-Organic Sodium Hybrid Capacitor: A New, High-Energy, High-Power Energy Storage System Bridging Batteries and Capacitors

Ranjith Thangavel,[†] Karthikeyan Kaliyappan,[‡] Dae-Ung Kim,[†] Xueliang Sun,[‡] and Yun-Sung Lee*[,†]

[†]Faculty of Applied Chemical Engineering, Chonnam National University, Gwang-ju 500-757, Korea

[‡]Department of Mechanical and Materials Engineering, University of Western Ontario, London, Ontario N6A 5B9, Canada

Supporting Information

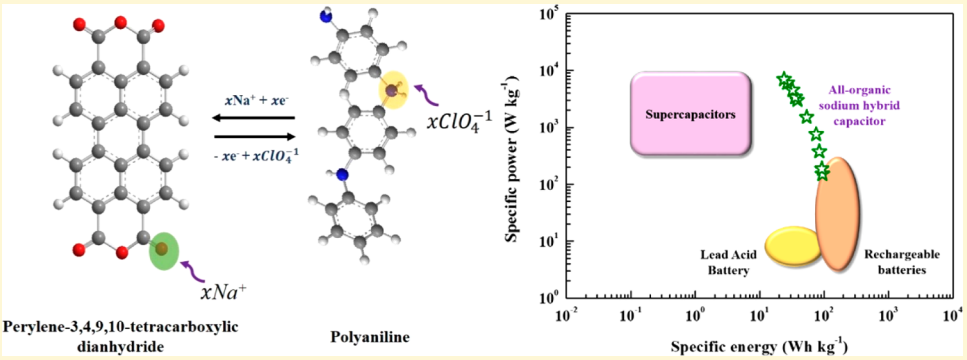

ABSTRACT: The development of hybrid capacitors (HCs) has become essential for meeting the rising demand for devices that simultaneously deliver high energy with high power. Although the challenge to develop high-performance HCs remains great, it is also simultaneously essential to develop an eco-friendly and cleaner energy storage system for sustainable future use. To date, hybrid capacitors utilize heavily toxic inorganic insertion electrodes and hazardous coke-derived porous carbon adsorption electrodes to host ions. Herein, we present a conceptually novel all-organic sodium hybrid capacitor (OHC), rationally designed by replacing the conventional electrodes with clean, green, and metal free organic molecules, to host ions. A high energy density of ~95 Wh kg^{-1} and an ultrahigh power density of 7 kW kg^{-1} (based on active mass in both electrodes) are achieved with a low energy loss of ~0.22% per 100 cycles (~89% retention after 5000 cycles), outperforming conventional HCs. The outstanding energy−power behavior of OHC bridges the performance gap between batteries and capacitors. This research holds great promise for the development of next-generation eco-friendly, clean, green, and safer high-energy, high-power devices.

1. INTRODUCTION

There is ever-increasing demand for smart energy storage devices in electric vehicles and large-scale power grids that must deliver high energy and high power along with a longer cycle life.[1,2] Because of their high energy density at high power along with their high cyclability, hybrid capacitors (HCs) have continued to gain prominence as next-generation energy storage systems for replacing low-power rechargeable batteries.[3−6] HCs possess a combination of two charge storage mechanisms: (i) intercalation/deintercalation in a battery type electrode and (ii) adsorption/desorption in an electric double-layer capacitor (EDLC) type electrode. Because of the merits of the two mechanisms, HCs simultaneously deliver high energy and high power.[7−10] The energy density of a packed hybrid capacitor device can exceed ~20 Wh kg^{-1}, which is nearly 3 times higher than that of conventional double-layer capacitors.

Although lithium hybrid capacitors have reached a commercial level of success, depletion of lithium resources has diverted the focus of research to sodium-based energy storage systems.[11−14] Very recently, sodium hybrid capacitors (NHCs) that outperform their lithium analogues have been reported. For example, metal oxides like Nb_2O_5, and WO_3 delivered high energy densities of 43.2 and 67 Wh kg^{-1}, respectively, emerging as a rival to lithium hybrid capacitors. A variety of metal oxides such as V_2O_5, $NiCo_2O_4$, and TiO_2 intercalation compounds, including $Na_3V_3(PO_4)_3$, $NaTi_2(PO_4)_3$, Mxenes, and $NaMn_{1/3}Co_{1/3}Ni_{1/3}PO_4$, have shown progressively improving performance.[11,15−20] However, addressing the sustainability and versatility of the high-performance hybrid capacitor systems becomes very crucial with growing concern about rapid climate change and global warming.[21,22]

To date, HCs use toxic transition metal-containing battery electrodes and environmentally hazardous coke-derived porous capacitor electrodes. Replacing the toxic conventional electrodes with green and eco-friendly compounds to host ions can ensure sustainability of NHCs.[11,23−25] However, this approach has not yet been realized in capacitor systems. Replacing the

Received: February 27, 2017
Revised: July 31, 2017
Published: July 31, 2017

DOI: 10.1021/acs.chemmater.7b00841
Chem. Mater. 2017, 29, 7122−7130

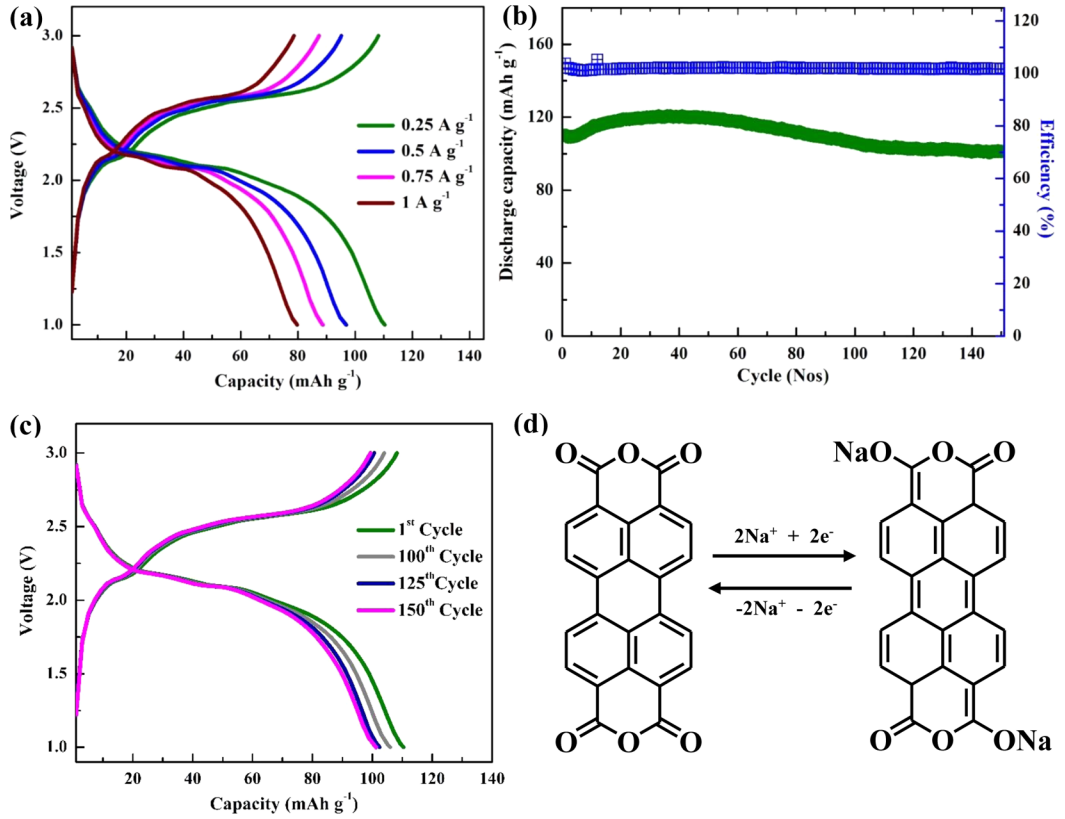

Figure 1. (a) Charge−discharge profile of PTCD at various current densities. (b) Cycling stability of PTCD at a current density of 0.25 A g^{-1}. (c) CD curves of PTCD at different cycles (0.25 A g^{-1}). (d) Sodium ion storage mechanism in PTCD.

inorganic sodium insertion electrodes and porous adsorption electrode in NHCs with organic hosts can facilitate the implementation of a conceptually new next-generation energy storage system with all-organic hybrid capacitors (OHCs), which could be widely structurally flexible and environmentally sustainable.[26−29]

In the conventional battery electrode of NHCs, charge storage occurs via reversible intercalation of sodium ion into the battery electrode, wherein a change in the oxidation state of the transition metal stabilizes the structure.[26,30,31] The transition metals in battery electrodes are highly toxic and inorganic complexes that require an environmentally harmful and highly complex extraction process. Furthermore, the inorganic complexes are depletable resources, and their synthesis consumes a large amount of energy.[26,32] Replacing the toxic compounds with highly abundant, metal free, and bioinspired organic molecules can provide a versatile stage for the development of green energy storage devices.[32,33]

A large number of organic compounds with redox-active sites have been successfully employed as hosts for sodium ions in organic sodium ion batteries.[6,34−36] The storage of sodium ion in organic molecules is primarily based on C═O reaction, doping reaction, and C═N reaction. Carbonyl reactions (C═O) are prevalent in carboxylate, quinone, imide, and anhydride compounds. Organic radicals, organometallics, and microporous polymers undergo doping reactions, while Schiff base and pteridine derivatives undergo C═N reactions.[34−36] In the search for an efficient candidate to host Na ions in OHCs, perylene-3,4,9,10-tetracarboxylic acid dianhydride (PTCD) has emerged as a judicious choice because of its multiple sodium ion bonding sites, which leads to high capacity.[37−39] The sodium ions can easily be incorporated into the aromatic rings of PTCD by a simple enolation process with no structural expansion.[37,40] Furthermore, the commercial availability of perylene could encourage its practical implementation in large-scale energy storage systems.

However, shortcomings such as the poor electrical conductivity, slow redox kinetics, high solubility in electrolyte, and poor rate capability of the organic molecule must be seriously addressed, when it is employed in a fast-working, high-power capacitor device. Strategies such as incorporating the organic hosts onto a highly conductive carbon host and embedding the organic molecules into a carbon network have been adapted to enhance the reaction kinetics and cycle life. Various types of conductive carbons, including CMK, ketjen black, graphene, and acetylene black, have recently been studied.[25,32−35] Therefore, PTCD molecules must be coupled with a highly conductive carbon support to realize a high level of energy retention under high-power conditions.[32−35]

In the case of a capacitor type electrode, highly porous activated carbon derived from coal and petroleum coke has been commercially used.[41−44] However, its high-temperature environmentally hazardous activation process and the low availability of fossil fuels limit the practical usage of activated carbon.[45] Furthermore, poor electronic conductivity and pore blockage impede the kinetics of ion storage under high-current conditions, thereby undermining the power output.[3,8] At higher currents, the poor ion transport inside the deeper pores leads to disproportionate capacitance, thereby curtailing the high output power.[46,47]

As an effective approach for developing efficient materials for hosting anions for OHCs, the strategy of accommodating

DOI: 10.1021/acs.chemmater.7b00841
Chem. Mater. 2017, 29, 7122−7130

anions by utilizing conducting polymers appears to be feasible. Despite their excellent performance in supercapacitors, the performance of conducting polymers in HCs has not been widely investigated. Among the various available polymers, electronically conductive polyaniline (PANI) is a popular choice. Unlike porous carbon that stores ions by double-layer formation at the electrode−electrolyte interface, conducting polymers store ions through a pseudocapacitive reaction.[48] In the protonated state, PANI efficiently stores anions through quick surface pseudocapacitance and is thus advantageous for achieving high energy even at high power versus double-layer-based carbon electrodes.[48−50] Additionally, the electronic conductivity and tailored nanostructure morphology of PANI can be easily controlled with reaction conditions.[51] Pseudocapacitance anionic storage by PANI offers further advantages of being inexpensive, being lightweight, and having excellent structural flexibility.[52−54]

Herein, we introduce a conceptually novel, all-organic hybrid capacitor (OHC) constructed with PTCD as a sodium insertion host and PANI as an anionic host. The new OHC delivers a maximum energy density of ∼95 Wh kg^{-1} (based on the active mass of both electrodes) and an ultrahigh power density of 7 kW kg^{-1}. Furthermore, a robust stability of ∼89% after 5000 cycles (0.22% loss of performance per 100 cycles) is achieved, evidence of this OHC outperforming traditional hybrid capacitors and sodium ion capacitors. This novel approach should initiate a new research trend toward the development of organic hybrid capacitors as prospective next-generation energy storage systems.

2. RESULTS AND DISCUSSION

Commercial PTCD was directly used for analysis without further processing. The X-ray diffraction (XRD) patterns of PTCD in Figure S1a indicate that PTCD was in the crystalline β-form in the monoclinic $P2_{1/c}$ space group. Structural investigation by field emission scanning electron microscopy (Figure S1b) revealed the rodlike morphology of PTCD, formed by agglomeration of submicrometer-sized particles. The extended conjugated structure of PTCD is highly beneficial for the enhanced electronic conductivity of PTCD electrodes. PTCD can insert two sodium ions into their structure with good structural reversibility.[37,55]

The as-synthesized PANI displayed a wormlike morphology with well-interconnected nanosized particles (Figure S1c). The well-connected PANI could greatly reduce the interparticle resistance and increase the electron transfer capability of the nanostructure. The Fourier transform infrared (FT-IR) spectrum in Figure S1d shows two strong characteristic peaks at ∼1575 and 1482 cm^{-1} due to stretching vibrations of the quinoid and benzenoid rings, respectively, confirming identification of the emeraldine form.[56] The deconvoluted N 1s core-level spectra of PANI from XPS studies (Figure S2) show three major components at ∼398.5, 399.2, and 401 eV, corresponding to quinoid imine (−N═), benzoind amine (−N−), and positively charged nitrogen (N^+), respectively.[51] The nitrogen adsorption−desorption isotherm of PANI indicated a large surface area of ∼35 m^2 g^{-1} with a hysteresis in the high-partial pressure region, confirming that mesopores are the major pore constituents (Figure S2). The mesoporous nature of PANI is highly beneficial for improving ion transport within the particles, and enhances the high power kinetics of OHC by the reversible pseudocapacitance reaction.[57,58]

2.1. Half-Cell Performance. Figure 1a shows the electrochemical performance of PTCD in the range of 1−3 V versus Na at different currents. The sloppy plateaus indicate sequential insertion and extraction of two Na^+ ions into and from the PTCD molecule, respectively, where the storage mechanism involves a redox reaction of the carboxyl groups through an enolation process.[37,59−61] A recent study reveals the possibility of insertion of up to 15 sodium ions into the PTCD structure between 0 and 3 V versus Na (sodium insertion takes place inside fused aromatic rings). However, with a high degree of insertion of sodium into the PTCD structure, the crystallinity and stability of PTCD are severely affected, so to maintain good reversibility in the capacitor device, PTCD was purposefully reduced only to dianion.[37] At 0.25 A g^{-1}, PTCD delivered a discharge capacity of ∼110 mAh g^{-1}, corresponding to the insertion into the carboxyl groups of nearly two sodium ions. Even at 1 A g^{-1}, a high discharge capacity of ∼80 mAh g^{-1} was achieved, indicative of excellent rate capability and superior structural stability at higher currents. Given that its structure is less rigid than that of inorganic compounds, PTCD exhibits a high affinity for electrons, thereby enabling high sodium mobility within the conjugated structure.[22,37] In addition, PTCD gave rise to a relatively low capacity decay with near ∼99% Coulombic efficiency even after 150 cycles at 0.25 A g^{-1} (Figure 1b,c). The scheme of the sodium ion storage mechanism in PTCD is given in Figure 1d. CV analysis of PTCD in Figure S3 shows a series of sharp reduction peaks between ∼1.8 and 2.1 V, corresponding to the insertion of sodium into the PTCD molecule, and the inserted sodiums are extracted back during the anodic scan at ∼2.6 V. The redox peaks obtained correlate with CD curves and previous reports.[37] The CV curves of PTCD after cycling show some changes compared to CV curves recorded before cycling. During the cathodic scan, the three consecutive peaks initially present become integrated into one broad peak with a negligible change in faradic current. During the anodic scan, the appearance of new peaks is noted with a small decrease in the faradic current. This difference in the shape profile of CV curves indicates that there might be a change in the PTCD material and charge transfer mechanism. Despite this change, the electrochemical properties of PTCD are maintained well with good retention of capacity over 150 cycles.

The effect of the conductive carbon additive is also studied on the PTCD organic compound. Although the pristine PTCD without a carbon support undergoes a nearly two-electron reaction during initial cycles with a capacity of ∼90 mAh g^{-1}, the number of sodiums taken up and capacity retention decrease with cycling because of the high resistance between the active materials without a carbon support (Figure S4).[60,61] This has been overcome by the ketjen black carbon support, and the conductive carbon content strongly influences the Coulombic efficiency and rate performance of the PTCD molecule (Figure S5). With an increase in the level of the carbon support, the use of active material is greatly enhanced at higher current rates, delivering a high capacity because of the improvement in electrical conductivity between the particles.[60] However, with an increase in carbon content, a slight decrease in Coulombic efficiency is noted. At higher carbon contents (20 wt %), the initial Coulombic efficiency is unstable and becomes stable after cycling. The contribution of ketjen black to PTCD is negligible and is shown in Figure S6.

The less rigid structure of PTCD can easily accommodate the large sodium ions, and the fast sodium kinetics inside the

DOI: 10.1021/acs.chemmater.7b00841
Chem. Mater. 2017, 29, 7122−7130

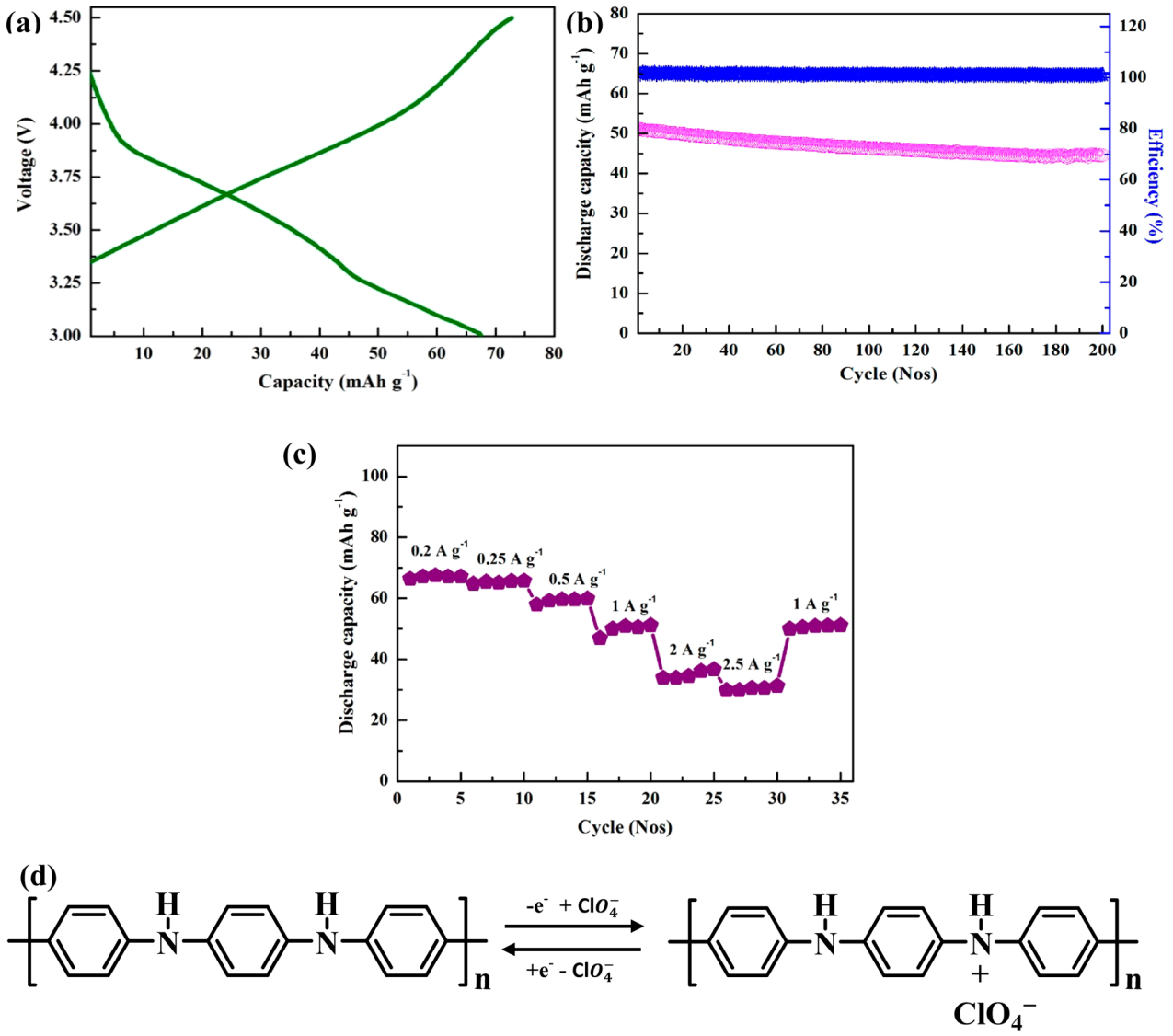

Figure 2. (a) Charge−discharge profile of PANI vs Na in the range of 3−4.5 V at 0.25 A g^{-1}. (b) Cycling stability of PANI at 1 A g^{-1}. (c) Rate performance of PANI. (d) Anion storage mechanism in PANI.

structure are highly favorable in terms of maximum sodium storage under high-current conditions in a hybrid capacitor.[37] The superior performance of PTCD, including the high reversible capacity, long stability, and high rate capability, is highly competitive with respect to those of many previously reported carbon and inorganic sodium anodes, thereby confirming that organic compounds could be an efficient alternative for hosting sodium ions in OHCs.

Figure 2a displays the electrochemical performance of PANI in the range of 3−4.5 V versus Na^+/Na. The charge−discharge (CD) curves are not linear given that the major storage mechanism is the pseudocapacitive reaction of the ClO_4^- anion through a fast reversible reaction.[62] The occurrence of such a fast pseudocapacitive reaction is highly advantageous for accommodating a large number of anions in a short time, thereby simultaneously boosting the energy density at higher powers. A discharge capacity of ∼68 mAh g^{-1} was delivered at 0.25 A g^{-1}, which is much higher than that obtained with porous carbon adsorption electrodes.[63] PANI delivered a superior rate performance of ∼51 mAh g^{-1} at a high discharge capacity of 1 A g^{-1} with an extremely high stability, where ∼100% Coulombic efficiency and ∼90% of the initial capacity was maintained beyond 200 cycles (Figure 2b). The excellent rate performance and capacity recovery (Figure 2c) confirm that PANI could be an efficient anionic host for high-power, high-energy OHCs. The scheme for pseudocapacitance anionic storage of PANI is given in Figure 2d. The performance of PANI in anionic storage is quite attractive, and surface pseudocapacitance storage is quite helpful in overcoming the diffusion limitations inside micropores of porous carbon electrodes at high powers.[64] The inherent electrical conductivity and the quick pseudocapacitance synergistically contribute to the higher capacity and superior rate capability. The deconvoluted N 1s core-level XPS spectra of PANI after cycling (Figure S7) show the presence of the positively charged nitrogen (N^+) component at ∼401.1 eV, confirming the stable and nondegradable chemical nature of PANI with repeated cycling. The quinoid imine (−N═) and benzoind amine (−N−) components are centered around ∼399 and 400.1 eV, respectively, and an only slight deviation from their original position with cycling was noted. The pseudocapacitive reaction does not induce any chemical degradation of the polymer

DOI: 10.1021/acs.chemmater.7b00841
Chem. Mater. 2017, 29, 7122−7130

chains; thus, the redox sites remain very active with cycling and could ensure the longevity of OHCs.[65,66]

2.2. All-Organic Hybrid Capacitor. The profile of the cyclic voltammetry (CV) curve of the OHC in the range of 0−3 V (Figure 3a) was not perfectly rectangular, deviating from

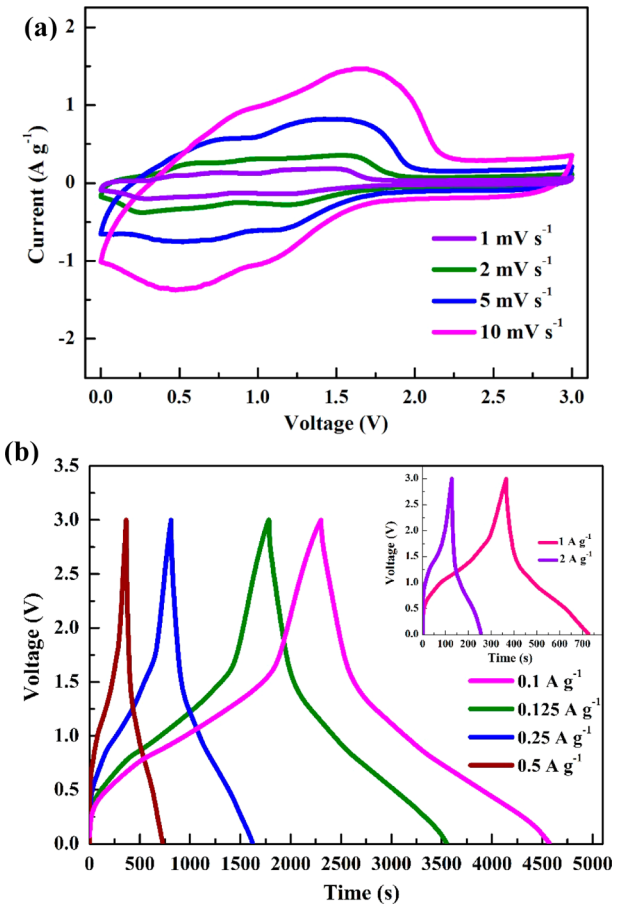

Figure 3. (a) Cyclic voltammetry curves of OHC. (b) Charge−discharge profile of OHC at various current densities. The inset shows the CD profile at 1 and 2 A g^{-1}.

shape linearity. The broad irregular redox peaks confirm the operation of two different energy storage mechanisms, making the OHC a hybrid energy storage device.[11] Even with an increase in the scan rate, the shape of the CV curves of the OHC was well retained, indicating its durability due to efficient and effective utilization of the active materials.

The profiles of the CD curves of the OHC (Figure 3b) do not conform to the typical rectangular shape because of the synergetic effect between the two charge storage mechanisms; the proposed charge storage mechanism for the OHC is presented in Figure 4. During charging, sodium ions are inserted into the carboxyl groups of PTCD by a redox reaction to form sodium enolate, and this is counterbalanced by simultaneous anion storage on PANI by a quick surface pseudocapacitance reaction; both of these processes are reversed on discharge. The shape of the CD curve of OHC was maintained even at high current rates, implying superior rate capability. The capacitance of the OHC cell was approximately 76, 73, 68, 61, 43, 31, 22, and 19 F g^{-1} at 0.1, 0.125, 0.25, 0.5, 1, 2, 4, and 4.7 A g^{-1} (Figure S8), respectively, and this novel OHC demonstrated an excellent electrochemical stability of ~89% even after 5000 robust cycles at 2.25 A g^{-1}

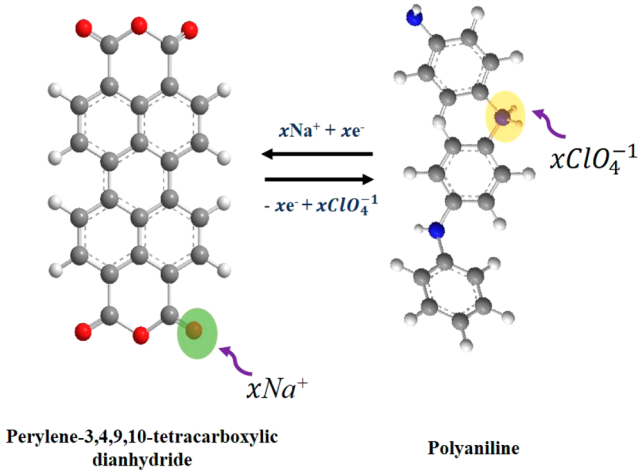

Figure 4. Scheme of the working principle of the OHC.

(Figure 5a,b). An ultralow performance fading of 0.22% per 100 cycles was documented, where the excellent stability is mainly

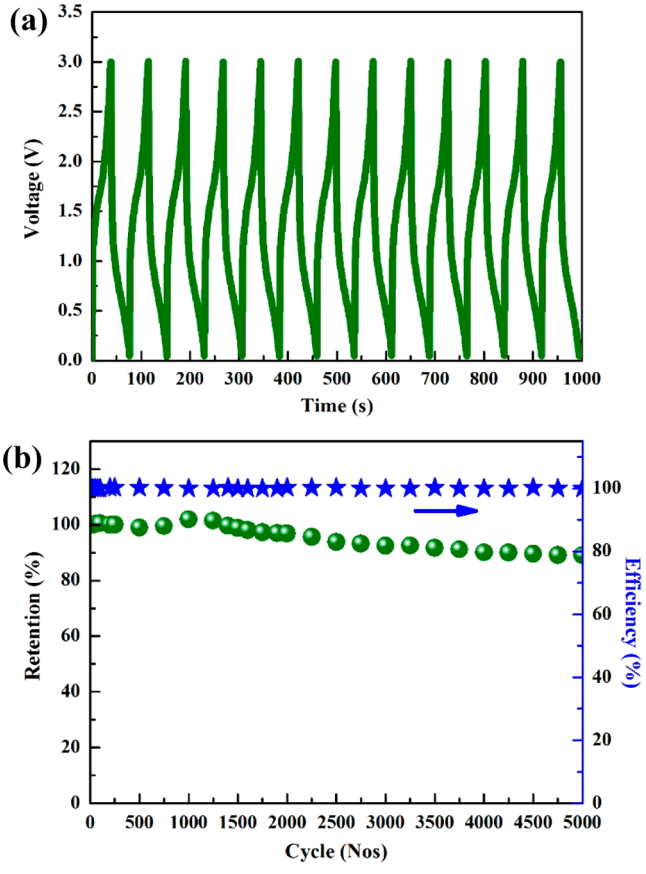

Figure 5. (a) Continuous charge−discharge curves of OHC at 2.25 A g^{-1}. (b) Cycling stability of the OHC.

ascribed to the robust structural stability of the organic molecules, as previously elucidated from the half-cell performance. The stability achieved with the OHC is much higher than that achieved with the battery system, where continuous deterioration of the active material in the latter affects the cycling performance.[5,67] The EDLC performance of ketjen black was also evaluated and is shown in Figure S9. Figure S9 shows that the conductive carbon in the electrode material not

DOI: 10.1021/acs.chemmater.7b00841
Chem. Mater. 2017, 29, 7122−7130

only altered the inherent conductive nature of the electrode materials but also significantly assisted in enhancing the overall capacitance and stability of the OHC.

The origin of this superior performance of the OHC can be explained by the impedance spectrum of the OHC before and after cycling (Figure S10). The Nyquist plots showed a semicircle in the high-frequency region occurring due to charge transfer at the electrode−electrolyte interface and an inclined profile in the low-frequency region occurring due to a diffusion-controlled process.[68,69] Only a minor change in the solution resistance and the electrode−electrolyte interface resistance was detected, implying that the electrode surface is highly active and readily available for reaction even after 5000 deep charge−discharge cycles.

The energy density and power density of the OHC were calculated from the discharge time and are presented in the Ragone plot in Figure 6a, illustrating that the OHC delivered a

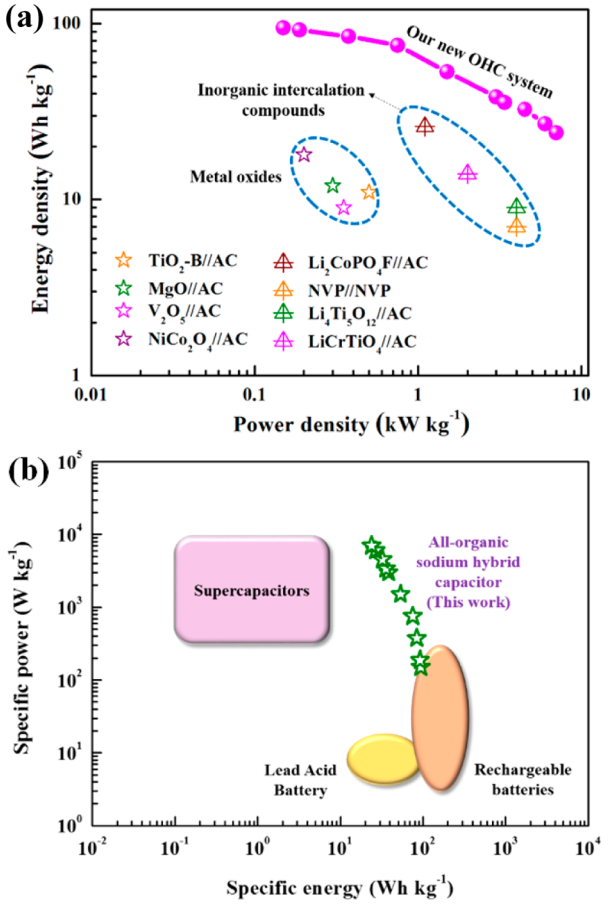

Figure 6. (a) Ragone plot for the OHC and comparison with inorganic hybrid capacitor systems. (b) Ragone plot comparing the OHC with other energy storage systems.

maximum energy density of ~95 Wh kg^{-1} (based on the active mass in both electrodes). Even at an ultrahigh power density of 7 kW kg^{-1}, where many HCs fail to deliver a high specific energy, the OHC could still deliver an energy density of ~24 Wh kg^{-1}. This output specific energy provides evidence that the OHC outperforms traditional hybrid capacitors that utilize inorganic metal oxides and intercalation compounds as anionic insertion hosts (Figure 6a).[62,70] The capability to function efficiently at a high power rate reveals the superiority of the OHC over batteries. The specific power and the specific energy retention at high power achieved with the OHC are superior to those of hybrid capacitor systems that utilize porous carbon adsorption electrodes by several orders of magnitude.[12,71−73] Furthermore, the OHC showed an ultralow performance fading per cycle even under high-power conditions compared to that of conventional HCs, thereby emerging as a competitive alternative candidate for electric vehicles and power grid applications.

Such a large energy output at a high specific power is made possible by utilizing PANI as an anionic host, where the quick pseudocapacitance is favorable for storage of large anions at higher current rates, whereas conventional ACs fail under these conditions; the reaction is kinetically counterbalanced by the large number of sodium ions inserted into the PTCD. Furthermore, the performance of the OHC was comprehensively compared with that of other systems as shown in Figure 6a, demonstrating that the OHC is far superior to conventional inorganic hybrid capacitor systems, including $Li_4Ti_4O_{12}$//AC, graphite//AC, TiO_2//AC, Nb_2O_5//AC, V_2O_5/AC, $Na_2Ti_3O_7$//AC, NVP//NVP, and many other systems documented in the literature.[4,11,12,16,19,74,75] Figure S11 compares the working scheme of OHNC and conventional HCs. Table S1 compares the output performance of the current OHC with those of previously reported lithium/sodium hybrid capacitors and ion capacitors. It clearly depicts the superiority of OHC versus other capacitors in terms of energy and power output. Replacing the toxic inorganic compounds makes the current system more sustainable for practical applications. The simultaneous high-power and high-energy behavior of the OHC bridges rechargeable batteries and supercapacitors (Figure 6b), and the OHC has emerged as a possible next-generation energy storage device. Moreover, on the basis of this performance, the conceptually novel OHC is a promising candidate for next-generation energy storage devices, meeting the requirements for powering future electric vehicles more efficiently and safely.

The superior performance of the OHC is mainly attributed to (i) the multiring conjugated structure of perylene that favors quick and reversible storage of a large number of sodium ions, (ii) the less rigid crystal structure of perylene formed by strong hydrogen bonding, which favors fast sodium insertion and extraction and provides good stability against the electrolyte, (iii) the pseudocapacitive storage on PANI that facilitates storage of a large number of anions, aiding the retention of the high specific energy even at high specific powers, and (iv) the inherent ultrahigh electrical conductivity and mesopores of PANI that synergistically function to overcome the sluggish kinetics of the ions by reducing their interfacial surface resistance and charge transfer resistance.

3. CONCLUSIONS

In summary, a novel, metal free, green energy storage system, i.e., an all-organic hybrid capacitor, was developed by utilizing the commercially available, green, and safe electrode materials, 3,4,9,10-tetracarboxylic acid dianhydride and PANI. This new OHC delivers a high energy density of ~95 Wh kg^{-1} and can withstand an ultrahigh power of 7 kW kg^{-1}. Moreover, this new OHC demonstrates excellent stability over 5000 cycles with ~89% performance retention, outperforming conventional hybrid capacitors that utilize inorganic compounds and porous carbon as the ionic host. This new OHC maintains an ultrahigh energy density without compromising the power density and thereby bridges the performance gap between electrical double-

DOI: 10.1021/acs.chemmater.7b00841
Chem. Mater. 2017, 29, 7122−7130

layer capacitors and batteries. This new approach opens a new gateway of research for utilizing organic ionic hosts in hybrid capacitor applications as a safe, green, and sustainable next-generation energy storage device.

4. EXPERIMENTAL SECTION

4.1. Polyaniline Synthesis. Polyaniline fibers were synthesized by a chemical polymerization technique using an aniline monomer (Sigma-Aldrich) and ammonium persulfate (Sigma-Aldrich) oxidizer in aqueous HCl medium.[51,54] The 0.2 M aniline monomer was first dissolved in 0.2 M aqueous HCl, and the chemical polymerization was imitated by addition of ammonium persulfate to the solution described above. All reactions were performed under ice bath conditions with continuous stirring. The resultant product was then thoroughly washed with distilled water and ethanol several times to remove any residual impurities and then dried under vacuum at 60 °C.

4.2. Characterization of Materials. X-ray diffraction (XRD) patterns of all powdered samples were collected on a Rigaku Rint 1000 diffractometer, utilizing Cu Kα radiation. Morphologies of the powdered samples were observed using a Hitachi S4700 field emission scanning electron microscope. FT-IR spectra were recorded on an IRPresitge-21 spectrometer. XPS data were recorded with a Multilab 2000 instrument using monochromatized Al Ka radiation (hn = 1486.6 eV). Nitrogen adsorption and desorption isotherms were performed using a Micromeritics ASAP 2010 surface analyzer.

4.3. Electrochemical Measurement. To evaluate the electrochemical performance, the following electrode composition was used: (i) PTCD electrode, 70 wt % active material, 15 wt % conductive additive (ketjen black), and 10 wt % binder (teflonized acetylene black); and (ii) PANI electrode, 80 wt % active material, 10 wt % conductive additive (ketjen black), and 10 wt % binder (teflonized acetylene black). The slurry was then rolled and pressured over a stainless steel mesh and dried at 90 °C for 12 h under vacuum prior to coin-cell fabrication. The electrodes were assembled in a standard CR2032 coin-cell inside an argon-filled glovebox with a moisture content of <0.1 ppm. The hybrid capacitor was assembled in a similar fashion, and the mass balance between the two electrodes was set at ~1:1.5 and the mass loading maintained at ~2.5 mg cm^{-2}. Porous polypropylene film was used as the separator, and $NaClO_4$ in a 1:1 (v/v) ethylene carbonate/dimethyl carbonate electrolyte was used. Cyclic voltammetry (CV) and electrochemical impedance spectroscopy (EIS) analyses of the OHC were performed using a Bio-Logic model SP-150 electrochemical workstation. Galvanostatic charge−discharge studies were performed with a Won-A-Tech cycler. The power density is calculated as $P = IV/2$ W kg^{-1}, where I is the current normalized by the active mass in both electrodes (amperes per gram) and V is the working potential of the system (volts). The energy density is calculated as $E = Pt$ Wh kg^{-1}, where t is the discharge time.

■ ASSOCIATED CONTENT

Supporting Information

The Supporting Information is available free of charge on the ACS Publications website at DOI: 10.1021/acs.chemmater.7b00841.

XRD pattern of PTCD, scanning electron microscopy (SEM) image of PTCD, FT-IR spectrum of PANI, SEM image of PANI, core-level N 1s XPS spectra of PANI, N_2 adsorption/desorption isotherm of PANI, CV curves of PTCD before and after cycling, cyclic stability of PTCD without a carbon support, effect of conductive carbon content in PTCD, half-cell performance of ketjen black versus Na, core-level N 1s XPS spectra of PANI after cycling, capacitance versus current density plot of the OHC, performance of the ketjen black EDLC capacitor, impedance plot of the OHC recorded before and after cycling, comparison of the performance of the OHC with conventional HCs, and a comparison of the performance of our new OHC with those of previously reported HCs (PDF)

■ AUTHOR INFORMATION

Corresponding Author

*E-mail: leeys@chonnam.ac.kr.

ORCID

Xueliang Sun: 0000-0003-2881-8237

Yun-Sung Lee: 0000-0002-6676-2871

Notes

The authors declare no competing financial interest.

■ ACKNOWLEDGMENTS

This work was supported by a National Research Foundation of Korea (NRF) grant funded by the Korea government (Ministry of Science, ICT & Future Planning) (2016R1A4A1012224).

■ REFERENCES

(1) Kang, K.; Meng, Y. S.; Bréger, J.; Grey, C. P.; Ceder, G. Electrodes with High Power and High Capacity for Rechargeable Lithium Batteries. *Science* **2006**, *311*, 977−980.

(2) Bruce, P. G.; Freunberger, S. A.; Hardwick, L. J.; Tarascon, J.-M. Li-O2 and Li-S batteries with high energy storage. *Nat. Mater.* **2012**, *11*, 19−29.

(3) Dubal, D. P.; Ayyad, O.; Ruiz, V.; Gomez-Romero, P. Hybrid energy storage: the merging of battery and supercapacitor chemistries. *Chem. Soc. Rev.* **2015**, *44*, 1777−1790.

(4) Aravindan, V.; Gnanaraj, J.; Lee, Y.-S.; Madhavi, S. Insertion-Type Electrodes for Nonaqueous Li-Ion Capacitors. *Chem. Rev.* **2014**, *114*, 11619−11635.

(5) Liu, C.; Li, F.; Ma, L.-P.; Cheng, H.-M. Advanced Materials for Energy Storage. *Adv. Mater.* **2010**, *22*, E28−E62.

(6) Ellis, B. L.; Nazar, L. F. Sodium and sodium-ion energy storage batteries. *Curr. Opin. Solid State Mater. Sci.* **2012**, *16*, 168−177.

(7) Yi, R.; Chen, S.; Song, J.; Gordin, M. L.; Manivannan, A.; Wang, D. High-Performance Hybrid Supercapacitor Enabled by a High-Rate Si-based Anode. *Adv. Funct. Mater.* **2014**, *24*, 7433−7439.

(8) Zhang, F.; Zhang, T.; Yang, X.; Zhang, L.; Leng, K.; Huang, Y.; Chen, Y. A high-performance supercapacitor-battery hybrid energy storage device based on graphene-enhanced electrode materials with ultrahigh energy density. *Energy Environ. Sci.* **2013**, *6*, 1623−1632.

(9) Li, H.; Zhu, Y.; Dong, S.; Shen, L.; Chen, Z.; Zhang, X.; Yu, G. Self-Assembled Nb2O5 Nanosheets for High Energy−High Power Sodium Ion Capacitors. *Chem. Mater.* **2016**, *28*, 5753−5760.

(10) Li, H.; Peng, L.; Zhu, Y.; Zhang, X.; Yu, G. Achieving High-Energy−High-Power Density in a Flexible Quasi-Solid-State Sodium Ion Capacitor. *Nano Lett.* **2016**, *16*, 5938−5943.

(11) Thangavel, R.; Kaliyappan, K.; Kang, K.; Sun, X.; Lee, Y.-S. Going Beyond Lithium Hybrid Capacitors: Proposing a New High-Performing Sodium Hybrid Capacitor System for Next-Generation Hybrid Vehicles Made with Bio-Inspired Activated Carbon. *Adv. Energy Mater.* **2016**, *6*, 1502199.

(12) Ding, J.; Wang, H.; Li, Z.; Cui, K.; Karpuzov, D.; Tan, X.; Kohandehghan, A.; Mitlin, D. Peanut shell hybrid sodium ion capacitor with extreme energy-power rivals lithium ion capacitors. *Energy Environ. Sci.* **2015**, *8*, 941−955.

(13) Kim, J.; Park, I.; Kim, H.; Park, K.-Y.; Park, Y.-U.; Kang, K. Tailoring a New 4V-Class Cathode Material for Na-Ion Batteries. *Adv. Energy Mater.* **2016**, *6*, 1502147.

(14) Thangavel, R.; Moorthy, B.; Kim, D. K.; Lee, Y.-S. Pushing the Energy Output and Cyclability of Sodium Hybrid Capacitors at High Power to New Limits. *Adv. Energy Mater.* **2017**, *7*, 1602654.

(15) Lim, E.; Jo, C.; Kim, M. S.; Kim, M.-H.; Chun, J.; Kim, H.; Park, J.; Roh, K. C.; Kang, K.; Yoon, S.; Lee, J. High-Performance Sodium-Ion Hybrid Supercapacitor Based on Nb2O5@Carbon Core−Shell

DOI: 10.1021/acs.chemmater.7b00841
Chem. Mater. 2017, 29, 7122−7130

Nanoparticles and Reduced Graphene Oxide Nanocomposites. *Adv. Funct. Mater.* **2016**, *26*, 3711−3719.
(16) Chen, Z.; Augustyn, V.; Jia, X.; Xiao, Q.; Dunn, B.; Lu, Y. High-Performance Sodium-Ion Pseudocapacitors Based on Hierarchically Porous Nanowire Composites. *ACS Nano* **2012**, *6*, 4319−4327.
(17) Wang, X.; Kajiyama, S.; Iinuma, H.; Hosono, E.; Oro, S.; Moriguchi, I.; Okubo, M.; Yamada, A. Pseudocapacitance of MXene nanosheets for high-power sodium-ion hybrid capacitors. *Nat. Commun.* **2015**, *6*, 6544.
(18) Kim, M. S.; Lim, E.; Kim, S.; Jo, C.; Chun, J.; Lee, J. General Synthesis of N-Doped Macroporous Graphene-Encapsulated Mesoporous Metal Oxides and Their Application as New Anode Materials for Sodium-Ion Hybrid Supercapacitors. *Adv. Funct. Mater.* **2017**, *27*, 1603921.
(19) Dong, S.; Shen, L.; Li, H.; Pang, G.; Dou, H.; Zhang, X. Flexible Sodium-Ion Pseudocapacitors Based on 3D Na2Ti3O7 Nanosheet Arrays/Carbon Textiles Anodes. *Adv. Funct. Mater.* **2016**, *26*, 3703−3710.
(20) Saravanan, K.; Mason, C. W.; Rudola, A.; Wong, K. H.; Balaya, P. The First Report on Excellent Cycling Stability and Superior Rate Capability of Na3V2(PO4)3 for Sodium Ion Batteries. *Adv. Energy Mater.* **2013**, *3*, 444−450.
(21) Schon, T. B.; McAllister, B. T.; Li, P.-F.; Seferos, D. S. The rise of organic electrode materials for energy storage. *Chem. Soc. Rev.* **2016**, *45*, 6345−6404.
(22) Miroshnikov, M.; Divya, K. P.; Babu, G.; Meiyazhagan, A.; Reddy Arava, L. M.; Ajayan, P. M.; John, G. Power from nature: designing green battery materials from electroactive quinone derivatives and organic polymers. *J. Mater. Chem. A* **2016**, *4*, 12370−12386.
(23) Wang, S.; Wang, L.; Zhu, Z.; Hu, Z.; Zhao, Q.; Chen, J. All Organic Sodium-Ion Batteries with Na4C8H2O6. *Angew. Chem.* **2014**, *126*, 6002−6006.
(24) Sun, T.; Li, Z.-j.; Wang, H.-g.; Bao, D.; Meng, F.-l.; Zhang, X.-b. A Biodegradable Polydopamine-Derived Electrode Material for High-Capacity and Long-Life Lithium-Ion and Sodium-Ion Batteries. *Angew. Chem., Int. Ed.* **2016**, *55*, 10662−10666.
(25) Lee, J.; Kim, H.; Park, M. J. Long-Life, High-Rate Lithium-Organic Batteries Based on Naphthoquinone Derivatives. *Chem. Mater.* **2016**, *28*, 2408−2416.
(26) Armand, M.; Grugeon, S.; Vezin, H.; Laruelle, S.; Ribiere, P.; Poizot, P.; Tarascon, J. M. Conjugated dicarboxylate anodes for Li-ion batteries. *Nat. Mater.* **2009**, *8*, 120−125.
(27) Yamashita, T.; Momida, H.; Oguchi, T. Crystal structure predictions of NaxC6O6 for sodium-ion batteries: First-principles calculations with an evolutionary algorithm. *Electrochim. Acta* **2016**, *195*, 1−8.
(28) Nesvadba, P.; Bugnon, L.; Maire, P.; Novák, P. Synthesis of A Novel Spirobisnitroxide Polymer and its Evaluation in an Organic Radical Battery. *Chem. Mater.* **2010**, *22*, 783−788.
(29) Itoi, H.; Yasue, Y.; Suda, K.; Katoh, S.; Hasegawa, H.; Hayashi, S.; Mitsuoka, M.; Iwata, H.; Ohzawa, Y. Solvent-free Preparation of Electrochemical Capacitor Electrodes Using Metal-free Redox Organic Compounds. *ACS Sustainable Chem. Eng.* **2017**, *5*, 556−562.
(30) Banda, H.; Damien, D.; Nagarajan, K.; Hariharan, M.; Shaijumon, M. M. A polyimide based all-organic sodium ion battery. *J. Mater. Chem. A* **2015**, *3*, 10453−10458.
(31) Fang, C.; Huang, Y.; Zhang, W.; Han, J.; Deng, Z.; Cao, Y.; Yang, H. Routes to High Energy Cathodes of Sodium-Ion Batteries. *Adv. Energy Mater.* **2016**, *6*, 1501727.
(32) Song, Z.; Zhou, H. Towards sustainable and versatile energy storage devices: an overview of organic electrode materials. *Energy Environ. Sci.* **2013**, *6*, 2280−2301.
(33) Nokami, T.; Matsuo, T.; Inatomi, Y.; Hojo, N.; Tsukagoshi, T.; Yoshizawa, H.; Shimizu, A.; Kuramoto, H.; Komae, K.; Tsuyama, H.; Yoshida, J.-i. Polymer-Bound Pyrene-4,5,9,10-tetraone for Fast-Charge and -Discharge Lithium-Ion Batteries with High Capacity. *J. Am. Chem. Soc.* **2012**, *134*, 19694−19700.
(34) Kim, H.; Kim, H.; Ding, Z.; Lee, M. H.; Lim, K.; Yoon, G.; Kang, K. Recent Progress in Electrode Materials for Sodium-Ion Batteries. *Adv. Energy Mater.* **2016**, *6*, 1600943.
(35) Kim, H.; Kwon, J. E.; Lee, B.; Hong, J.; Lee, M.; Park, S. Y.; Kang, K. High Energy Organic Cathode for Sodium Rechargeable Batteries. *Chem. Mater.* **2015**, *27*, 7258−7264.
(36) Wan, F.; Wu, X.-L.; Guo, J.-Z.; Li, J.-Y.; Zhang, J.-P.; Niu, L.; Wang, R.-S. Nanoeffects promote the electrochemical properties of organic Na2C8H4O4 as anode material for sodium-ion batteries. *Nano Energy* **2015**, *13*, 450−457.
(37) Luo, W.; Allen, M.; Raju, V.; Ji, X. An Organic Pigment as a High-Performance Cathode for Sodium-Ion Batteries. *Adv. Energy Mater.* **2014**, *4*, 1400554.
(38) Xu, F.; Wang, H.; Lin, J.; Luo, X.; Cao, S.-a.; Yang, H. Poly(anthraquinonyl imide) as a high capacity organic cathode material for Na-ion batteries. *J. Mater. Chem. A* **2016**, *4*, 11491−11497.
(39) Xing, Z.; Jian, Z.; Luo, W.; Qi, Y.; Bommier, C.; Chong, E. S.; Li, Z.; Hu, L.; Ji, X. A perylene anhydride crystal as a reversible electrode for K-ion batteries. *Energy Storage Mater.* **2016**, *2*, 63−68.
(40) Deng, W.; Shen, Y.; Qian, J.; Cao, Y.; Yang, H. A Perylene Diimide Crystal with High Capacity and Stable Cyclability for Na-Ion Batteries. *ACS Appl. Mater. Interfaces* **2015**, *7*, 21095−21099.
(41) Frackowiak, E.; Béguin, F. Carbon materials for the electrochemical storage of energy in capacitors. *Carbon* **2001**, *39*, 937−950.
(42) Zhang, L. L.; Zhao, X. S. Carbon-based materials as supercapacitor electrodes. *Chem. Soc. Rev.* **2009**, *38*, 2520−2531.
(43) Lozano-Castelló, D.; Cazorla-Amorós, D.; Linares-Solano, A.; Shiraishi, S.; Kurihara, H.; Oya, A. Influence of pore structure and surface chemistry on electric double layer capacitance in non-aqueous electrolyte. *Carbon* **2003**, *41*, 1765−1775.
(44) Kim, T.; Jung, G.; Yoo, S.; Suh, K. S.; Ruoff, R. S. Activated Graphene-Based Carbons as Supercapacitor Electrodes with Macro- and Mesopores. *ACS Nano* **2013**, *7*, 6899−6905.
(45) Thangavel, R.; Kaliyappan, K.; Ramasamy, H. V.; Sun, X.; Lee, Y.-S. Engineering Pores of Biomass-Derived Carbon: Insights for Achieving Ultra-high Stability at High Power in High-Energy Supercapacitors. *ChemSusChem* **2017**, *10*, 2805−2815.
(46) Eliad, L.; Salitra, G.; Soffer, A.; Aurbach, D. Ion Sieving Effects in the Electrical Double Layer of Porous Carbon Electrodes: Estimating Effective Ion Size in Electrolytic Solutions. *J. Phys. Chem. B* **2001**, *105*, 6880−6887.
(47) Kim, T. Y.; Lee, H. W.; Stoller, M.; Dreyer, D. R.; Bielawski, C. W.; Ruoff, R. S.; Suh, K. S. High-Performance Supercapacitors Based on Poly(ionic liquid)-Modified Graphene Electrodes. *ACS Nano* **2011**, *5*, 436−442.
(48) Bryan, A. M.; Santino, L. M.; Lu, Y.; Acharya, S.; D'Arcy, J. M. Conducting Polymers for Pseudocapacitive Energy Storage. *Chem. Mater.* **2016**, *28*, 5989−5998.
(49) Simon, P.; Gogotsi, Y. Materials for electrochemical capacitors. *Nat. Mater.* **2008**, *7*, 845−854.
(50) Liu, T.; Finn, L.; Yu, M.; Wang, H.; Zhai, T.; Lu, X.; Tong, Y.; Li, Y. Polyaniline and Polypyrrole Pseudocapacitor Electrodes with Excellent Cycling Stability. *Nano Lett.* **2014**, *14*, 2522−2527.
(51) Park, H.-W.; Kim, T.; Huh, J.; Kang, M.; Lee, J. E.; Yoon, H. Anisotropic Growth Control of Polyaniline Nanostructures and Their Morphology-Dependent Electrochemical Characteristics. *ACS Nano* **2012**, *6*, 7624−7633.
(52) Lee, K.; Cho, S.; Heum Park, S.; Heeger, A. J.; Lee, C.-W.; Lee, S.-H. Metallic transport in polyaniline. *Nature* **2006**, *441*, 65−68.
(53) Wang, Q.; Yan, J.; Dong, Z.; Qu, L.; Fan, Z. Densely stacked bubble-pillared graphene blocks for high volumetric performance supercapacitors. *Energy Storage Mater.* **2015**, *1*, 42−50.
(54) Yang, J.; Yu, C.; Liang, S.; Li, S.; Huang, H.; Han, X.; Zhao, C.; Song, X.; Hao, C.; Ajayan, P. M.; Qiu, J. Bridging of Ultrathin NiCo2O4 Nanosheets and Graphene with Polyaniline: A Theoretical and Experimental Study. *Chem. Mater.* **2016**, *28*, 5855−5863.
(55) Luo, C.; Wang, J.; Fan, X.; Zhu, Y.; Han, F.; Suo, L.; Wang, C. Roll-to-roll fabrication of organic nanorod electrodes for sodium ion batteries. *Nano Energy* **2015**, *13*, 537−545.

DOI: 10.1021/acs.chemmater.7b00841
Chem. Mater. 2017, 29, 7122−7130

(56) Furukawa, Y.; Ueda, F.; Hyodo, Y.; Harada, I.; Nakajima, T.; Kawagoe, T. Vibrational spectra and structure of polyaniline. *Macromolecules* **1988**, *21*, 1297−1305.
(57) D'Arcy, J. M.; El-Kady, M. F.; Khine, P. P.; Zhang, L.; Lee, S. H.; Davis, N. R.; Liu, D. S.; Yeung, M. T.; Kim, S. Y.; Turner, C. L.; Lech, A. T.; Hammond, P. T.; Kaner, R. B. Vapor-Phase Polymerization of Nanofibrillar Poly(3,4-ethylenedioxythiophene) for Supercapacitors. *ACS Nano* **2014**, *8*, 1500−1510.
(58) Largeot, C.; Portet, C.; Chmiola, J.; Taberna, P.-L.; Gogotsi, Y.; Simon, P. Relation between the Ion Size and Pore Size for an Electric Double-Layer Capacitor. *J. Am. Chem. Soc.* **2008**, *130*, 2730−2731.
(59) Wang, H.-g.; Yuan, S.; Si, Z.; Zhang, X.-b. Multi-ring aromatic carbonyl compounds enabling high capacity and stable performance of sodium-organic batteries. *Energy Environ. Sci.* **2015**, *8*, 3160−3165.
(60) Jaffe, A.; Saldivar Valdes, A.; Karunadasa, H. I. Quinone-Functionalized Carbon Black Cathodes for Lithium Batteries with High Power Densities. *Chem. Mater.* **2015**, *27*, 3568−3571.
(61) Wang, C.; Fang, Y.; Xu, Y.; Liang, L.; Zhou, M.; Zhao, H.; Lei, Y. Manipulation of Disodium Rhodizonate: Factors for Fast-Charge and Fast-Discharge Sodium-Ion Batteries with Long-Term Cyclability. *Adv. Funct. Mater.* **2016**, *26*, 1777−1786.
(62) Karthikeyan, K.; Amaresh, S.; Lee, S.-N.; An, J.-Y.; Lee, Y.-S. High-Power Lithium-Ion Capacitor using LiMnBO3-Nanobead Anode and Polyaniline-Nanofiber Cathode with Excellent Cycle Life. *ChemSusChem* **2014**, *7*, 2310−2316.
(63) Huang, J.; Sumpter, B. G.; Meunier, V. Theoretical Model for Nanoporous Carbon Supercapacitors. *Angew. Chem., Int. Ed.* **2008**, *47*, 520−524.
(64) Song, W.-L.; Li, X.; Fan, L.-Z. Biomass derivative/graphene aerogels for binder-free supercapacitors. *Energy Storage Mater.* **2016**, *3*, 113−122.
(65) Wang, K.; Wu, H.; Meng, Y.; Wei, Z. Conducting Polymer Nanowire Arrays for High Performance Supercapacitors. *Small* **2014**, *10*, 14−31.
(66) Song, Y.; Liu, T.-Y.; Xu, X.-X.; Feng, D.-Y.; Li, Y.; Liu, X.-X. Pushing the Cycling Stability Limit of Polypyrrole for Supercapacitors. *Adv. Funct. Mater.* **2015**, *25*, 4626−4632.
(67) Naoi, K.; Ishimoto, S.; Miyamoto, J.-i.; Naoi, W. Second generation 'nanohybrid supercapacitor': Evolution of capacitive energy storage devices. *Energy Environ. Sci.* **2012**, *5*, 9363−9373.
(68) Shan, X.-Y.; Wang, Y.; Wang, D.-W.; Li, F.; Cheng, H.-M. Armoring Graphene Cathodes for High-Rate and Long-Life Lithium Ion Supercapacitors. *Adv. Energy Mater.* **2016**, *6*, 1502064.
(69) Karthick, R.; Brindha, M.; Selvaraj, M.; Ramu, S. Stable colloidal dispersion of functionalized reduced graphene oxide in aqueous medium for transparent conductive film. *J. Colloid Interface Sci.* **2013**, *406*, 69−74.
(70) Kim, H.; Park, K.-Y.; Cho, M.-Y.; Kim, M.-H.; Hong, J.; Jung, S.-K.; Roh, K. C.; Kang, K. High-Performance Hybrid Supercapacitor Based on Graphene-Wrapped Li4Ti5O12 and Activated Carbon. *ChemElectroChem* **2014**, *1*, 125−130.
(71) Wang, H.; Mitlin, D.; Ding, J.; Li, Z.; Cui, K. Excellent energy-power characteristics from a hybrid sodium ion capacitor based on identical carbon nanosheets in both electrodes. *J. Mater. Chem. A* **2016**, *4*, 5149−5158.
(72) Wang, R.; Lang, J.; Zhang, P.; Lin, Z.; Yan, X. Fast and Large Lithium Storage in 3D Porous VN Nanowires−Graphene Composite as a Superior Anode Toward High-Performance Hybrid Supercapacitors. *Adv. Funct. Mater.* **2015**, *25*, 2270−2278.
(73) Liu, C.; Zhang, C.; Song, H.; Zhang, C.; Liu, Y.; Nan, X.; Cao, G. Mesocrystal MnO cubes as anode for Li-ion capacitors. *Nano Energy* **2016**, *22*, 290−300.
(74) Karthikeyan, K.; Amaresh, S.; Kim, K. J.; Kim, S. H.; Chung, K. Y.; Cho, B. W.; Lee, Y. S. A high performance hybrid capacitor with Li2CoPO4F cathode and activated carbon anode. *Nanoscale* **2013**, *5*, 5958−5964.
(75) Wang, H.; Guan, C.; Wang, X.; Fan, H. J. A High Energy and Power Li-Ion Capacitor Based on a TiO2 Nanobelt Array Anode and a Graphene Hydrogel Cathode. *Small* **2015**, *11*, 1470−1477.

DOI: 10.1021/acs.chemmater.7b00841
Chem. Mater. 2017, 29, 7122−7130